

Voltage tunability of single spin-states in a quantum dot

Anthony J. Bennett,^{1,*} Matthew A. Pooley,^{1,2} Yameng Cao,^{1,3}
Niklas Sköld,¹ Ian Farrer,² David A. Ritchie,² and Andrew J. Shields¹

¹*Toshiba Research Europe Limited, Cambridge Research Laboratory,
208 Science Park, Milton Road, Cambridge, CB4 0GZ, U. K.*

²*Cavendish Laboratory, Cambridge University,
J. J. Thomson Avenue, Cambridge, CB3 0HE, U. K.*

³*Department of Physics, Imperial College London,
Prince Consort Road, London SW7 2AZ, U. K.*

(Dated: July 28, 2018)

Single spins in the solid-state offer a unique opportunity to store and manipulate quantum information, and to perform quantum-enhanced sensing of local fields and charges. Optical control of these systems using techniques developed in atomic physics has yet to exploit all the advantages of the solid-state. We demonstrate voltage tunability of the spin energy levels in a single quantum dot by modifying how spins sense magnetic field. We find the in-plane g -factor varies discontinuously for electrons, as more holes are loaded onto the dot. In contrast, the in-plane hole g -factor varies continuously. The device can change the sign of the in-plane g -factor of a single hole, at which point an avoided crossing is observed in the two spin eigenstates. This is exactly what is required for universal control of a single spin with a single electrical gate.

PACS numbers:

The spin of charges in quantum dots (QDs) has long been considered a suitable qubit for quantum operations [1]. The three dimensional confinement offered by a single semiconductor QD reduces many decoherence mechanisms, allowing impressively long coherence times to be observed in coherent population trapping [2] or using spin-echo techniques [3, 4]. In the latter, control of the spins was achieved with resonant, ultrafast optical pulses. An alternative mechanism for controlling single spins is for an electric field to vary their coupling to a fixed magnetic field (\mathbf{B}), described by the g -tensor (\mathbf{g}) [5]. This method allows multiple closely spaced spin qubits to be individually addressed via nano-electrodes, without resonant lasers or localised magnetic fields. Critical to this concept is the ability to change the sign of one component of the g -tensor [5, 6]. Then through careful alignment of the magnetic field direction it is possible to switch between two electric fields where the precession directions of the spin (given by $\mathbf{g}\cdot\mathbf{B}$) are orthogonal on the Bloch sphere. In such a system ‘universal’ control can map any point on the Bloch sphere onto any other point. Although experimental studies have been made of the g -tensor in QDs [7–12], the change of sign of one component with electrical field has yet to be reported.

Early work used semiconductor quantum wells to electronically tune the g -tensor of multiple spins by shifting their carrier wavefunctions into areas of different material composition [13]. Extending this work to single charges trapped in zero-dimensional structures has not been straightforward as the carriers tunnel out of the

structure when electric field is applied.

One approach was demonstrated using electronically coupled pairs of QDs [14]. Carriers displayed the g -tensor of the material in which they were located, so when a voltage was applied to localise the charge in one dot the g -factor measured was that of the indium-rich QD. However, when the wavefunction was delocalised between the dots there was a much greater spatial overlap with AlAs semiconductor in the barrier, and a change in g was observed.

Recently, experiments showed that vertical electric fields can change the g -factor relevant for out-of-plane magnetic fields (g^\perp) [9] in dots that are engineered to have increased height and reduced indium-composition. The in-plane g -factor of an s -shell hole ($g_{h,s}^\parallel$) was also modified by vertical electric field [10] over a modest field range of 20 kV/cm. However, both of these measurements were made in the photo-current regime, where carriers rapidly tunnel from the dot greatly limiting the spin lifetime. Conversely, an in-plane electric field can change the g -tensor but there the tunneling problem is even more severe [11, 12].

We solve these problems by locating single dots in the center of a $p-i-n$ diode where barriers that hinder tunneling allow us to apply electric fields, F , up to -500 kV/cm, whilst still observing photoluminescence [15]. We study changes in the g -tensor as a function of electric field and show a high degree of control can be achieved for both electrons and holes. We observe that continuous variation in the g -factor of holes in a parallel magnetic field can be obtained. Different behavior is observed depending on whether the hole is in the s - or p -shell. When $g_{h,s}^\parallel$ has a low value at zero electric field these devices are capable of tuning it through an avoided crossing at finite field, and changing its sign, without carriers escaping.

*Electronic address: anthony.bennett@crl.toshiba.co.uk; Corresponding author

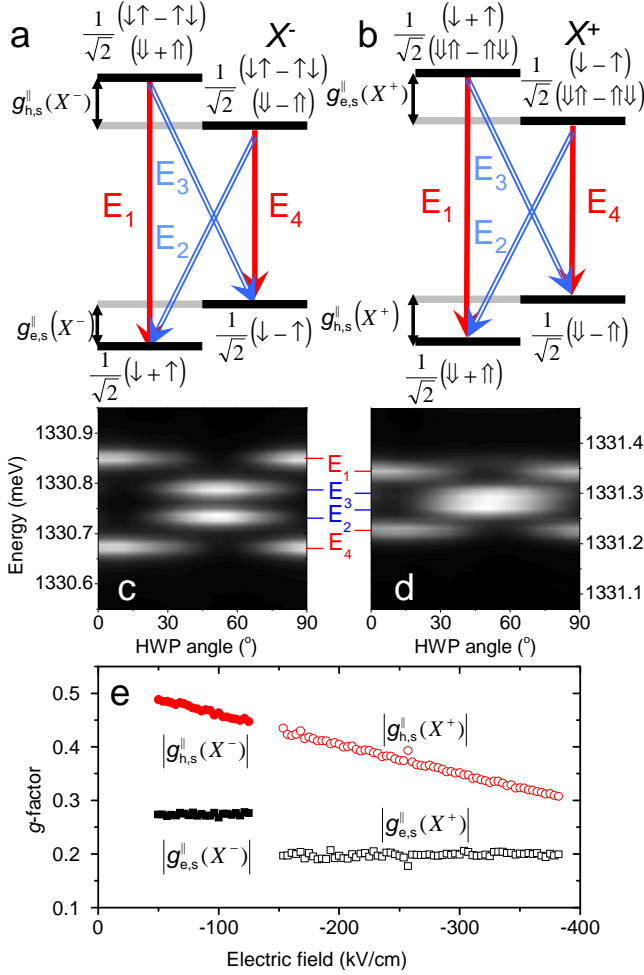


FIG. 1: **Electric field tuning of s -shell electron and hole g -factors** (a) and (b) show the energy levels of the negatively and positively charged excitons (X^- and X^+ , respectively) in a Voigt geometry magnetic field. Transitions E_1 and E_4 (red) result in linearly polarised emission orthogonal to the magnetic field and E_2 and E_3 (blue) are parallel to the magnetic field. (c) and (d) show polarisation dependent spectra from the X^- at -78.5 kV/cm and X^+ at -385.7 kV/cm (respectively) at a field of 4T, as a half wave plate (HWP) is rotated. (e) shows the extracted s -shell electron g -factor, $|g_{e,s}^{\parallel}|$, and s -shell hole g -factor, $|g_{h,s}^{\parallel}|$, as a function of electric field.

Results

Charged exciton transitions in magnetic and electric field. When the magnetic field is orthogonal to the plane of the sample (Faraday geometry, B^\perp) we see that the g -factors are barely affected by electric field (see Supplementary Figure S1 and Supplementary Notes). However, when the magnetic field is aligned in the plane of the sample (Voigt geometry, B^\parallel) strikingly different behavior is observed. The separate in-plane g -factors of an s -shell electrons ($g_{e,s}^{\parallel}$) and holes ($g_{h,s}^{\parallel}$) may be de-

termined from the decay energies of the positively (X^+) and negatively (X^-) charged excitons. The magnetic field splits both the upper ($g_{h,s}^{\parallel}\mu_B B^\parallel$) and lower states ($g_{e,s}^{\parallel}\mu_B B^\parallel$) of X^- , where μ_B is the Bohr Magnetron. Four transitions (E_1 to E_4) are observed as shown in Figure 1a,b. The highest and lowest energy transitions of this quadruplet (E_1 and E_4) emit photons with electric field orthogonal to \mathbf{B} and the intermediate transitions (E_2 and E_3) parallel to \mathbf{B} . Fitting the energies of each transition resulting from the X^- state one can determine $g_{e,s}^{\parallel}(X^-)$ and $g_{h,s}^{\parallel}(X^-)$ using $g_{e,s}^{\parallel}(X^-)\mu_B B^\parallel = E_1 - E_3 = E_2 - E_4$ and $g_{h,s}^{\parallel}(X^-)\mu_B B^\parallel = E_1 - E_2 = E_3 - E_4$. Similar arguments can be made to determine $g_{e,s}^{\parallel}(X^+)$ and $g_{h,s}^{\parallel}(X^+)$ from the X^+ transitions. There is not enough information in this measurement alone to determine the sign of these g -factors. However, for nearly all dots we see an increase in the fine-structure splitting of the neutral exciton state with magnetic field, which is a signature that both have the same sign [16], which we take to be negative [14, 17].

$g_{e,s}^{\parallel}$ appears to be constant for a given exciton complex, but on switching between the X^+ and X^- transitions an abrupt step is always observed. The reason for this is that $g_{e,s}^{\parallel}(X^+)$ is determined by the initial state (when there are two holes also present in the dot). These holes are better confined than the electron and provide a coulomb attraction that reduces the extent of the electron wavefunction, pushing $g_{e,s}^{\parallel}$ closer to $+2$ [18]. However, $g_{e,s}^{\parallel}$ when no holes are present is determined from the final state of the X^- transition. For the sample of 15 dots studied $|g_{e,s}^{\parallel}(X^-)| = 0.266 \pm 0.012$ and $|g_{e,s}^{\parallel}(X^+)| = 0.178 \pm 0.033$, where the numbers quoted are the mean \pm the standard deviation.

In contrast to the behavior of the electron, $g_{h,s}^{\parallel}$ varies linearly with electric field for both X^+ and X^- in Fig. 1e. We estimate the discontinuity in $g_{h,s}^{\parallel}$ on switching between X^+ and X^- is on average an order of magnitude smaller than the similar effect for $g_{e,s}^{\parallel}$, as expected given the greater spatial extent of the electron wavefunction. There is remarkable homogeneity in the rate at which $g_{h,s}^{\parallel}$ can be tuned with electric field for different dots, $\xi = |dg_{h,s}^{\parallel}/dF| = (5.7 \pm 1.5) \times 10^{-4}$ cm/kV where $|g_{h,s}^{\parallel}|$ at zero electric field is 0.469 ± 0.110 . The scatter in the value of $g_{h,s}^{\parallel}$ at $F = 0$ is greater than the comparable value for the electron, as this is affected more strongly by variations in dot height and lateral size [18]. The rate ξ compares well with the recent publication of Godden *et al* [10] which determines $|g_{h,s}^{\parallel}|$ from the energy splitting of the X^- in a time-resolved photo-current measurement. This paper reports a linear variation in $g_{h,s}^{\parallel}$ at a rate of 3.5×10^{-4} cm/kV over a range of only 20 kV/cm. The

rate of shift is also of the same order of magnitude as that predicted theoretically, for dots of greater height and uniform composition[6]. It will be interesting to see whether further theoretical work can fully explain the variations in the g -tensor we observe.

Minimising the g -factor of the s -shell hole. With the range of fields accessible in these samples, any dot with $|g_{h,s}^{\parallel}| \leq 0.285$ at $F = 0$ can be tuned to a minimum $|g_{h,s}^{\parallel}|$ at some field, F_0 . We now discuss data from a dot with $|g_{h,s}^{\parallel}| = 0.174$ at $F = 0$. This same QD also displays a minimum in the fine-structure splitting of the neutral exciton of $1.8 \mu\text{eV}$ at -57.1 kV/cm . We find that $|dg_{h,s}^{\parallel}/dF| = 7.74 \times 10^{-4} \text{ cm/kV}$, and thus we are able to tune the hole eigenstate splitting $\Delta = |g_{h,s}^{\parallel}| \mu_B B$ towards a minimum value at an electric field of $F_0 = -225.0 \text{ kV/cm}$. For fields above F_0 (such as shown in Fig. 2a) we observe that the sign of $g_{h,s}^{\parallel}$ is the same as for all other dots in the ensemble. For electric fields below F_0 (such as in Fig. 2e) $g_{h,s}^{\parallel}$ has the opposite sign, which manifests itself as a clear difference in the orientation angle at which the largest difference in transition energies is observed. Fig. 2f plots the X^+ transition energies as a function of electric field, F , to clearly show the form of the anti-crossing in the hole states (the mean value of all four transition energies has been subtracted for clarity, to remove the Stark shift). The minimum hole state splitting corresponds to $|g_{h,s}^{\parallel}(F_0)| = 0.042$, but we stress that on either side of this minimum value the $g_{h,s}^{\parallel}$ has different sign.

The behavior of Δ is reminiscent of the anti-crossing in neutral exciton states that has been observed with electric field [15, 19, 20], however in this case the states that are coupled together contain only a single hole. Indeed, in the analysis of Plumhof *et al* [21], who studied the anti-crossing of the neutral exciton states under externally applied strain, it was the hole wavefunction that dominated the orientation of the eigenstates relative to the laboratory (θ) and anti-crossing of the eigenenergies. As with the neutral exciton we fit the avoided crossing with a coupling parameter $g_{h,s}^{\parallel}(F_0) \mu_B B^{\parallel}$, where the splitting between the hole states varies linearly away from F_0 at a rate $\xi \mu_B B^{\parallel}$.

$$\Delta = g_{h,s}^{\parallel}(F) \mu_B B^{\parallel} = \mu_B B^{\parallel} \sqrt{\xi^2 (F - F_0)^2 + (g_{h,s}^{\parallel}(F_0))^2} \quad (1)$$

$$\theta = \pm \tan^{-1} \left[\frac{g_{h,s}^{\parallel}(F_0)}{\xi (F - F_0) \pm g_{h,s}^{\parallel}(F)} \right] \quad (2)$$

In Fig. 2g and h we show data summarising the behavior of the two hole eigenstates at 4T (the lowest field at which we can spectrally resolve all four transitions) and 5T (the highest field available with our magnet) fitted with this model. We observe that the magnitude of the anti-crossing in energy appears to scale linearly with B^{\parallel} , thus $|g_{h,s}^{\parallel}(F_0)|$ is constant, at least in the range of fields we can probe. The resulting variation of θ with F is the same for both magnetic fields (Fig. 2h), in accordance with equations 1 and 2. It will be interesting to further probe the behavior of this effect in higher magnetic fields.

g -factor of the p -shell hole. Finally, we study the decay of the positively charged biexciton, XX^+ , which consists of a filled s -shell and a excess p -shell hole. These transitions are observed on the low energy side of the X^+ transition [22, 23]. We determine the g -factors of the p -shell hole which, to our knowledge, has not been possible before (although the Voigt geometry electron p -shell g -factor has been probed [24]). We find that in the Faraday geometry there is no variation in the p -shell hole g -factor as a function of electric field. In a Voigt geometry the brightest radiative decays from XX^+ involve recombination of an s -shell electron and hole. The resulting photons are linearly polarised as shown in Fig. 3a (blue and red arrows have orthogonal linear polarisation) with the initial state XX^+ split by $g_{h,p}^{\parallel} \mu_B B^{\parallel}$, where $g_{h,p}^{\parallel}$ is the Voigt p -shell hole g -factor. However, the final states can either have spin $S = 1/2$ or $5/2$: their splittings are partly determined by the electron-hole exchange between the s -shell electron and p -shell hole which has not been well studied. Empirically, we see that the spin splitting of the $S = 1/2$ final state is below the system resolution at $B^{\parallel} = 0$, but increases with magnetic field. In contrast, the $S = 5/2$ final state has a spin splitting of several hundred μeV at $B^{\parallel} = 0$ but is reduced with B^{\parallel} . Nevertheless, it is possible to measure the initial state splitting XX^+ , using either the $S = 1/2$ or $S = 5/2$ final state quadruplets, and thus infer $|g_{h,p}^{\parallel}|$. When this is done, both quadruplets lead to the same value of $|g_{h,p}^{\parallel}|$ (Fig. 3e), as expected. We find that $|g_{h,p}^{\parallel}|$ has a greater magnitude than $|g_{h,s}^{\parallel}|$ and varies non-linearly with electric field. The greater extent of the p -shell hole wavefunction outside the dot is likely to bring $g_{h,p}^{\parallel}$ closer to the value determined by the wetting layer and surrounding GaAs.

Discussion

Several proposals exist for universal control of a single spin in a QD [1, 5, 6, 25]. The ability of the device reported here to change the sign of $|g_{h,s}^{\parallel}|$, combined with the reduced hole-hyperfine interaction and greater hole

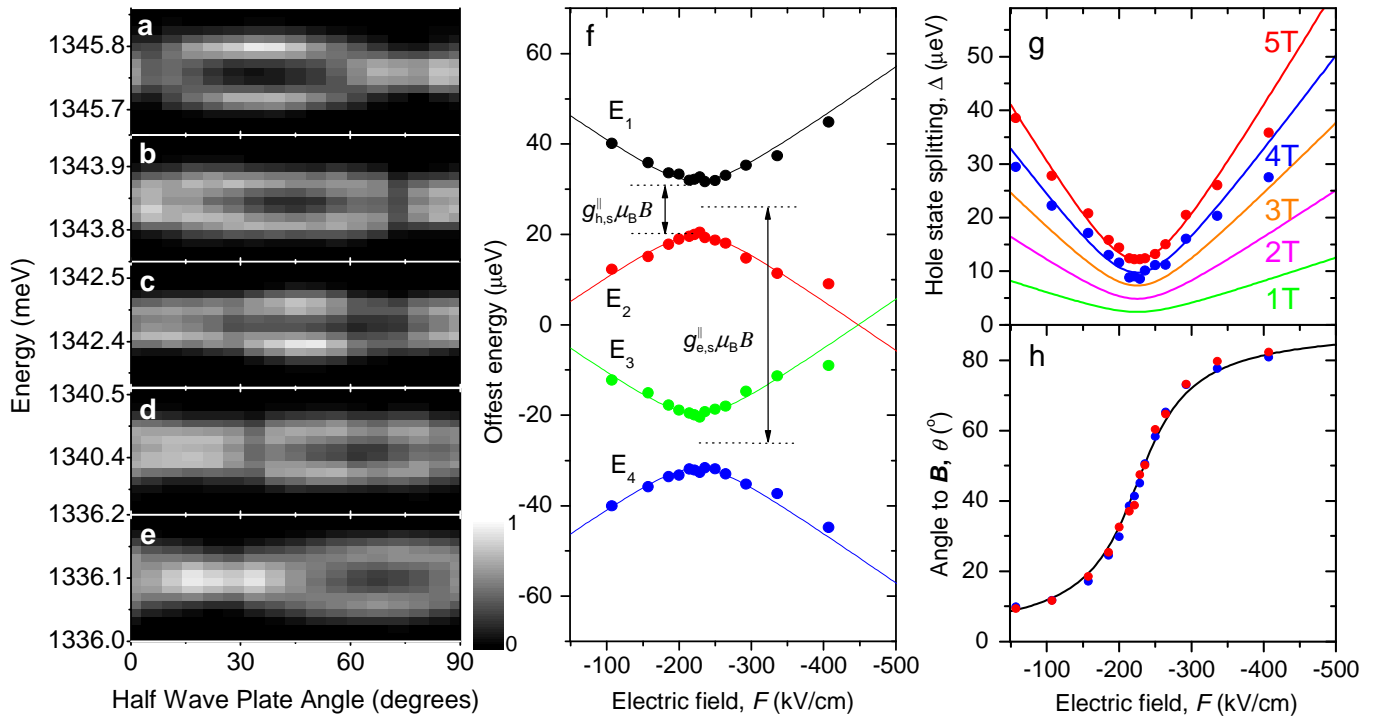


FIG. 2: **Changing the sign of the Voigt-geometry s -shell hole g -factor with electric field.** Polarized spectra of the positively-charged exciton X^+ , for an in-plane magnetic field of 5T and electric fields of (a) -107.1 kV/cm (b) -185.7 kV/cm (c) -221.4 kV/cm (d) -264.3 kV/cm and (e) -335.7 kV/cm. (f) shows the energies of the four transitions of the X^+ offset by their mean value at each electric field. (g) the magnitude of the hole g -factor, $|g_{h,s}^|||$ and the (h) orientation (θ) of the states relative to the magnetic field. Both (g) and (h) show fits for 1 to 5T based on equations 1 and 2

spin lifetime open up the possibility of all-electrical 4π manipulation of the hole spin. Alternatively, controlled phase shifts may be achieved on a qubit encoded on the spin of the electron by addition of two holes for a pre-determined time, which could be achieved by controlled charging.

The timescale of any electrical control sequence is limited by the resistance and capacitance of the diode to tens of picoseconds [26], which is significantly greater than that achieved with coherent optical pulses. However, the ability to achieve full Bloch-sphere control with only a single electrical gate is a promising avenue of investigation. Such a device could find applications in a spin-based quantum memory [27], spin-echo techniques [3, 4] spin based quantum computing [1, 28] and generation of photonic cluster-states [29].

Methods

Sample design. The sample consists of a single layer of self assembled quantum dots grown in the center of a 10nm wide GaAs quantum well, clad with a 75% AlGaAs superlattice which suppresses the tunneling of carriers. These dots are grown in a single deposition of InAs at

a substrate temperature of 470°C and with a transition to self-assembled 3D growth at 60 seconds. The resulting dots are 2-3nm in height, and are capped in 5nm of GaAs at 470°C before raising the substrate temperature for growth of the superlattice. p and n doping regions are arranged symmetrically above and below the QD layer, with a total intrinsic region thickness of 140 nm. The diode is encased in a weak planar microcavity, with micron sized apertures in a metallic layer on the surface to allow optical addressing of single dots.

Experimental arrangement. The sample is mounted inside the bore of a superconducting magnet applying fields of up to 5T. When the sample growth direction is aligned with the magnetic field a single on-axis microscope objective is used to excite and collect the emission from the sample. When the magnetic field is in the plane of the sample (Voigt Geometry) an additional 45° mirror is mounted to allow optical access to the sample. Photoluminescence is excited from the sample with a continuous wave 850 nm laser diode, and passed through a rotatable half-wave plate and polariser before detection. For the data in Fig. 2 spectral measurements confirm the sample was orientated within 0.1° of the magnetic field direction.

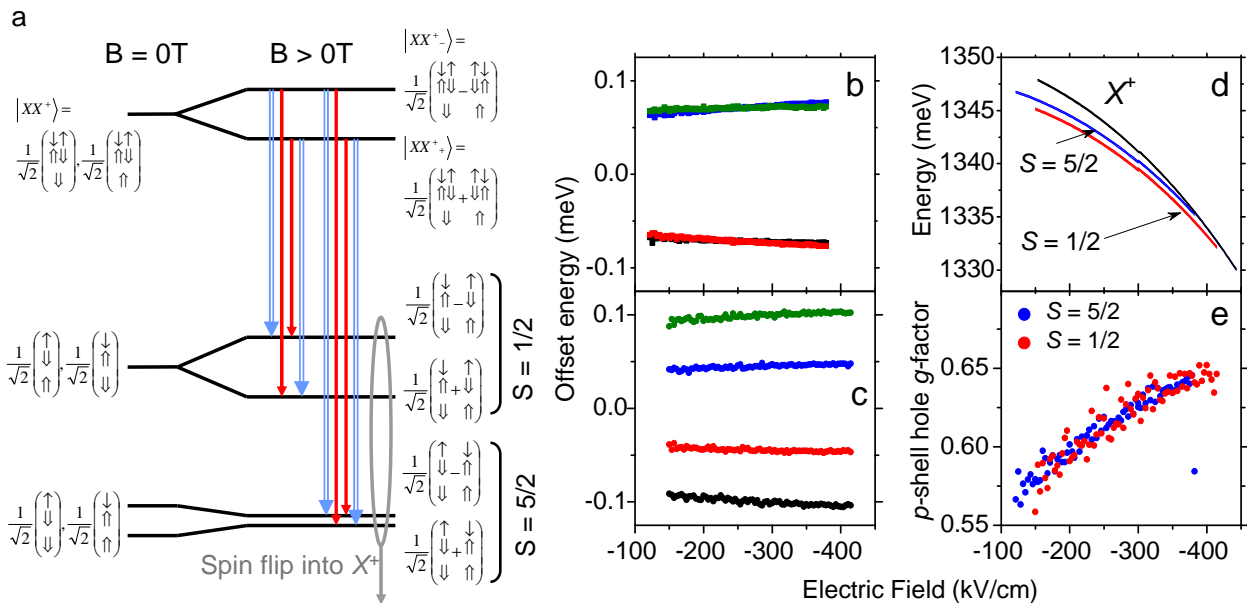


FIG. 3: **Determination of Voigt-geometry p -shell hole g -factor.** (a) shows the allowed transitions for recombination of an s -shell electron-hole pair of the positively-charged biexciton, XX^+ . Red and blue arrows indicate photon emission with opposite linear polarisation. (b) the energies of the quadruplet with $S = 5/2$ final state, offset by their mean at 4T, and (c) the energies of the quadruplet with $S = 1/2$ final state, offset by their mean at 4T, as a function of electric field. (d) shows the absolute energy of the transitions shown in (a) versus electric field, at 4T. From (b) and (c) we independently extract the magnitude of the p -shell hole g -factor (e) for the $S = 1/2$ (red) and $S = 5/2$ (blue) transitions.

Acknowledgements

This work was partly supported by the EU through the Integrated Project QESSENSE (project reference 248095), the Marie Curie Initial Training Network (ITN) ‘‘Spin-Optronics’’ (project number 237252) and EPSRC.

Author Contributions The samples were grown by I.F. and D.A.R., and processed by M.A.P. The optical measurements were made by A.J.B., M.A.P., Y.C. and N.S. A.J.S. guided the work. All authors discussed the results and their interpretation. A.J.B. wrote the manuscript, with contributions from the other authors.

Competing Financial Interests

The authors declare no competing financial interests.

Supplementary Information

We also carried out measurements of the Zeeman splittings in the Faraday geometry, where B^\perp is orientated out of the sample plane. The 4 brightest s -shell transitions, neutral exciton (X), biexciton (XX) and positively and negatively charged exciton (X^+ , X^-) are split into two components with opposite circular polarisation. When excited by a linearly polarised 850nm laser both circular polarisation components of each transition are visible in the spectrum (Figure 4b). The splitting of

each state is the same within error suggesting the presence of differing numbers of carriers does not change the sum of the Faraday s -shell electron and hole g -factors, $|g_{e,s}^\perp + g_{h,s}^\perp|$. The Zeeman splitting of X^- , shown in Figure 4c, is proportional to $|g_{e,s}^\perp + g_{h,s}^\perp| \mu_B B^\perp$. There is a 3% change in this splitting from -150 to -500 kV/cm (Figure 4d, filled data points).

From the Zeeman splitting observed with linearly polarised excitation we are only able to determine $|g_{e,s}^\perp + g_{h,s}^\perp|$, not the separate g -factors. However, optically pumping the system with a circularly polarised laser preferentially creates one sign of electron spin in the quantum dot. This imbalance of electron spin can partially polarise the nuclear field through an electron-flip/nuclear-flop process, resulting in an abrupt change in Zeeman splitting as the pump intensity is increased [30]. Above this critical pump intensity the Zeeman splitting is constant, because the nuclear field has been sufficiently polarised to counteract the effect of the magnetic external field. Now the Zeeman splitting is determined only by $|g_{h,s}^\perp|$ so the two g -factors can be determined separately. Measurements of the Zeeman splitting in the nuclear pumping regime are shown in Figure 4d as open data points, with nuclear pumping only possible at fields less than -150 kV/cm. Here the X^+ is dominant in the spectrum and it is the unpaired electron in the upper state that is polarising the nuclear field. Noise in the data means it is not possible to determine whether the

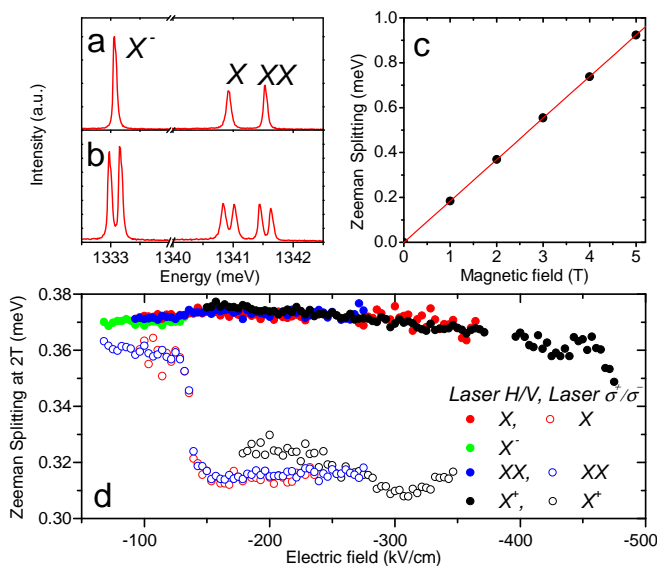


FIG. 4: : **Measurements of Faraday-geometry g -factors.** Emission spectrum at (a) 0T and (b) 1T, both for an electric field of -57.1 kV/cm. (c) the splitting of the negatively-charged exciton, X^- at -57.1 kV/cm, as the magnetic field is changed. (d) shows the Zeeman splitting of X^- , the neutral exciton (X), neutral-biexciton (XX) and positively-charged exciton (X^+), as a function of electric field. The closed circles indicate excitation with a linearly polarised laser, where the Zeeman splitting is proportional to the sum of the s -shell electron and hole g -factors, $|g_{e,s}^\perp + g_{h,s}^\perp|$, and the open data points with a circularly polarised laser sufficiently intense to partially polarise the nuclear field, leading to a splitting proportional to only the s -shell hole g -factor, $|g_{h,s}^\perp|$.

small variation in $|g_{e,s}^\perp + g_{h,s}^\perp|$ is due to $|g_{h,s}^\perp|$ or $|g_{e,s}^\perp|$. However, we infer that $|g_{e,s}^\perp| \sim 0.5$ and $|g_{h,s}^\perp| \sim 2.7$, over a bias range of several hundred kV/cm. These absolute values are consistent with previous reports working at lower electric fields, which take the sign of both g -factors to be negative.

-
- [1] D. Loss and D. P. DiVincenzo, Quantum computation with quantum dots, *Phys. Rev. A* **57**, 120-126 (1998)
- [2] Brunner, D. *et al*, A Coherent Single-Hole Spin in a Semiconductor, *Science*. **325**, 70-72 (2009)
- [3] Press, D. *et al*, Ultrafast optical spin echo in a single quantum dot, *Nature Photonics*. **4**, 307-311 (2010)
- [4] De Greve, K. *et al*, Ultrafast coherent control and suppressed nuclear feedback of a single quantum dot hole qubit, *Nature. Phys.* **7**, 872-878 (2011)
- [5] Pingenot, J., Pryor, C. E., and M. E. Flatté, M. E., Method for full Bloch sphere control of a localised spin via a single electrical gate, *Appl. Phys. Lett.* **92**, 222502 (2008)
- [6] Pingenot, J., Pryor, C. E., and M. E. Flatté, Electric-field manipulation of the Lande g tensor of a hole in an InGaAs/GaAs self-assembled quantum dot, *Phys. Rev. B* **84**, 195403 (2011)
- [7] Bayer, M *et al*, Fine structure of neutral and charged excitons in self-assembled InGaAs-AlGaAs quantum dots, *Phys. Rev. B* **65**, 195315 (1999).
- [8] Schwan, A. *et al*, Anisotropy of electron and hole g -factors in (In,Ga)As quantum dots., *Appl. Phys. Lett.* **99**, 221914 (2011)
- [9] Jovanov, V. *et al*, Observation and explanation of strong electrically tunable exciton g factors in composition engineered In(Ga)As quantum dots, *Phys. Rev. B* **83**, 161303 (R)(2011)
- [10] Godden, T. M. *et al*, Fast preparation of single hole spin in InAs/GaAs quantum dot in Voigt geometry magnetic field, *Phys. Rev. B* **85**, 155310 (2012)
- [11] Nakaoka, T., Tarucha, S., and Arakawa, Y., Electrical tuning of the g factor of single self-assembled quantum dots, *Phys. Rev. B* **76**, 041301 (2007)
- [12] Deacon, R. S. *et al*, Electrically tuned g tensor in an InAs self-assembled quantum dot, *Phys. Rev. B* **84**, 041302 (2011)
- [13] Salis, G. *et al*, Electrical control of spin coherence in semiconductor nanostructures, *Nature*. **414**, 619-621 (2001)
- [14] Doty, M. F. *et al*, Electrically Tunable g -Factors in Quantum Dot Molecular Spin States, *Phys. Rev. Lett.* **97**, 197202 (2006)
- [15] Bennett, A. J. *et al*, Electric field induced coherent coupling of the exciton states in a single semiconductor quantum dot, *Nature Phys.* **100**, 177401 (2010).
- [16] Stevenson, R. M. *et al*, Magnetic field induced reduction in the fine-structure splitting of InAs quantum dots, *Phys. Rev. B* **73**, 033306 (2006)

- [17] Xu, X *et al*, Fast spin initialization in a single charged InAs-GaAs quantum dot by optical cooling, *Phys. Rev. Lett.* **99**, 097401 (2007)
- [18] Pryor, C. E., and M. E. Flatté, Landé g factors and orbital angular momentum quenching in semiconductor quantum dots, *Phys. Rev. B* **96**, 026804 (2006).
- [19] Ghali, M., Ohtani, K., Ohno, Y. and Ohno, H., Generation and control of polarization-entangled photons from GaAs island quantum dots by an electric field, *Nature Comms.* **3**, 661 (2012).
- [20] Trotta, R. *et al*, Universal Recovery of the Energy-Level Degeneracy of Bright Excitons in InGaAs Quantum Dots without a Structure Symmetry, *Phys. Rev. Lett.* **109**, 147401 (2012).
- [21] Plumhof, J. *et al*, Strain induced anticrossing of the bright exciton levels in single self assembled quantum dots, *Phys. Rev. B* **83**, 121302 (2011).
- [22] Rodt, S., Schliwa, A., Ptschke, K., Guffarth, A., and Bimberg, D., Correlation of structural and few-particle properties of self-organized InAs GaAs quantum dots, *Phys. Rev. B* **71**, 155325 (2005)
- [23] Akimov, I. A., Hundt, A., Flissikowski, T. and Henneberger, F., Fine structure of the trion triplet state in a single self-assembled semiconductor quantum dot, *Appl. Phys. Lett.* **81**, 4730-4732 (2002)
- [24] Mayer Alegre, T. P., Hernandez, F. G. G., Pereira, A. L. C. and Medeiros-Ribero, G., Landé g tensor in semiconductor nanostructures, *Phys. Rev. Lett.* **97**, 236402 (2006)
- [25] Andlauer, T. and Vogl, P., Electrically controllable g tensors in quantum dot molecules, *Phys. Rev. B* **79**, 045307 (2009)
- [26] Bennett, A. J. *et al*, Indistinguishable photons from a diode, *Appl. Phys. Lett.* **100**, 207503 (2008)
- [27] Heiss, D. *et al*, Optically monitoring electron spin relaxation in a single quantum dot using a spin memory device, *Phys. Rev. B* **82**, 245316 (2010)
- [28] Foletti, S., Bluhm, H., Mahalu, O., Umansky, U. and Yacoby, A., Universal quantum control of two-electron spin quantum bits using dynamic nuclear polarization, *Nature Phys.* **5**, 903-908 (2009)
- [29] Lindner, N. H. and Rudolph, T., Proposal for Pulsed On-Demand Sources of Photonic Cluster State Strings, *Phys. Rev. Lett.* **103**, 113602 (2009)
- [30] Tartakovskii, A. I. *et al*, Nuclear Spin Switch in Semiconductor Quantum Dots, *Phys. Rev. Lett.* **98**, 026806 (2007).